REPORT DOCUMENTATION PAGE

Form Approved OMB NO. 0704-0188

The public reporting burden for this collection of information is estimated to average 1 hour per response, including the time for reviewing instructions, searching existing data sources, gathering and maintaining the data needed, and completing and reviewing the collection of information. Send comments regarding this burden estimate or any other aspect of this collection of information, including suggesstions for reducing this burden, to Washington Headquarters Services, Directorate for Information Operations and Reports, 1215 Jefferson Davis Highway, Suite 1204, Arlington VA, 22202-4302. Respondents should be aware that notwithstanding any other provision of law, no person shall be subject to any oenalty for failing to comply with a collection of information if it does not display a currently valid OMB control number.
PLEASE DO NOT RETURN YOUR FORM TO THE ABOVE ADDRESS.

1. REPORT DATE (DD-MM-YYYY)	2. REPORT TYPE	3. DATES COVERED (From - To)
	Technical Report	-

4. TITLE AND SUBTITLE	5a. CONTRACT NUMBER
THE ROLE OF METAL OXIDES IN NANOTHERMITE REACTIONS: EVIDENCE OF CONDENSED PHASE INITIATION	W911NF-09-1-0214
	5b. GRANT NUMBER
	5c. PROGRAM ELEMENT NUMBER
	611102

6. AUTHORS	5d. PROJECT NUMBER
N. W. Piekiel, K. T. Sullivan, S. Chowdhury, and M. R. Zachariah	
	5e. TASK NUMBER
	5f. WORK UNIT NUMBER

7. PERFORMING ORGANIZATION NAMES AND ADDRESSES	8. PERFORMING ORGANIZATION REPORT NUMBER
University of Maryland - College Park Research Admin. & Advancement University of Maryland College Park, MD 20742 -5141	

9. SPONSORING/MONITORING AGENCY NAME(S) AND ADDRESS(ES)	10. SPONSOR/MONITOR'S ACRONYM(S)
U.S. Army Research Office P.O. Box 12211 Research Triangle Park, NC 27709-2211	ARO
	11. SPONSOR/MONITOR'S REPORT NUMBER(S)
	55832-EG.2

12. DISTRIBUTION AVAILIBILITY STATEMENT

Approved for Public Release; Distribution Unlimited

13. SUPPLEMENTARY NOTES

The views, opinions and/or findings contained in this report are those of the author(s) and should not contrued as an official Department of the Army position, policy or decision, unless so designated by other documentation.

14. ABSTRACT

This work is a culmination of several corresponding studies designed to probe the initiation and reaction of aluminum nanothermite systems. The main diagnostic tool used in this study is a Temperature-Jump/Time-of-Flight Mass Spectrometer (T-Jump/TOFMS), which uses a filament heating method capable of very high heating rates up to 106 oC/s, while spectra are simultaneously obtained at a time resolution of 100 μs. Nanothermites of Al/CuO, Al/Fe2O3, Al/WO3, and Al/Bi2O3 were all tested with this system along with

15. SUBJECT TERMS

Nanoenergetic materials

16. SECURITY CLASSIFICATION OF:			17. LIMITATION OF ABSTRACT	15. NUMBER OF PAGES	19a. NAME OF RESPONSIBLE PERSON
a. REPORT	b. ABSTRACT	c. THIS PAGE			Michael Zachariah
UU	UU	UU	UU		19b. TELEPHONE NUMBER
					301-405-4311

Standard Form 298 (Rev 8/98)
Prescribed by ANSI Std. Z39.18

THE ROLE OF METAL OXIDES IN NANOTHERMITE REACTIONS: EVIDENCE OF CONDENSED PHASE INITIATION

ABSTRACT

This work is a culmination of several corresponding studies designed to probe the initiation and reaction of aluminum nanothermite systems. The main diagnostic tool used in this study is a Temperature-Jump/Time-of-Flight Mass Spectrometer (T-Jump/TOFMS), which uses a filament heating method capable of very high heating rates up to 106 oC/s, while spectra are simultaneously obtained at a time resolution of 100 μs. Nanothermites of Al/CuO, Al/Fe2O3, Al/WO3, and Al/Bi2O3 were all tested with this system along with the neat Al and metal oxide powders. High speed imaging was also used to visually compare reaction rates of each sample showing that, contradictory to some previous works, Al/Bi2O3 reacts much faster than the other nanothermites. The nanothermites Al/CuO, Al/Fe2O3, and Al/WO3 showed a correlation of ignition with the neat oxide's decomposition to gas phase products. However, the Al/Bi2O3 sample clearly ignites at a temperature well below the decomposition of Bi2O3 to gaseous products, which strongly suggests a condensed phase initiation mechanism for Al/Bi2O3. To further investigate this mechanism, C/Bi2O3 was also tested as, unlike aluminum, carbon will remain in the solid phase in the temperature regime of our experiments. This work showed similar results as the Al/Bi2O3 where C/Bi2O3 clearly reacts before Bi2O3 decomposes. In a complimentary study a high-heating rate TEM grid was also used to probe the behavior of individual nanoparticles under these experimental conditions. While testing Bi2O3 it was seen that the material reacted with the carbon coating of the TEM grid, again displaying a condensed phase reaction. The TEM studies provide evidence that other nanothermites may follow this mechanism as well. Furthermore, a T-Jump/PMT setup was used to optically determine the burn times and ignition temperatures in filament heating experiments, and was also used at the Argonne National Laboratory's Advanced Photon Source. This work provided unique high speed phase contrast imaging that offers further insight into the aluminum nanothermite reactions.

THE ROLE OF METAL OXIDES IN NANOTHERMITE REACTIONS: EVIDENCE OF CONDENSED PHASE INITIATION

N. W. Piekiel, K. T. Sullivan, S. Chowdhury, and M. R. Zachariah

Department of Mechanical Engineering and Department of Chemistry and Biochemistry
University of Maryland, College Park, MD
College Park, MD 20742

Abstract

This work is a culmination of several corresponding studies designed to probe the initiation and reaction of aluminum nanothermite systems. The main diagnostic tool used in this study is a Temperature-Jump/Time-of-Flight Mass Spectrometer (T-Jump/TOFMS), which uses a filament heating method capable of very high heating rates up to 10^6 ^{o}C/s, while spectra are simultaneously obtained at a time resolution of 100 μs. Nanothermites of Al/CuO, Al/Fe$_2$O$_3$, Al/WO$_3$, and Al/Bi$_2$O$_3$ were all tested with this system along with the neat Al and metal oxide powders. High speed imaging was also used to visually compare reaction rates of each sample showing that, contradictory to some previous works, Al/Bi$_2$O$_3$ reacts much faster than the other nanothermites. The nanothermites Al/CuO, Al/Fe$_2$O$_3$, and Al/WO$_3$ showed a correlation of ignition with the neat oxide's decomposition to gas phase products. However, the Al/Bi$_2$O$_3$ sample clearly ignites at a temperature well below the decomposition of Bi$_2$O$_3$ to gaseous products, which strongly suggests a condensed phase initiation mechanism for Al/Bi$_2$O$_3$. To further investigate this mechanism, C/Bi$_2$O$_3$ was also tested as, unlike aluminum, carbon will remain in the solid phase in the temperature regime of our experiments. This work showed similar results as the Al/Bi$_2$O$_3$ where C/Bi$_2$O$_3$ clearly reacts before Bi$_2$O$_3$ decomposes. In a complimentary study a high-heating rate TEM grid was also used to probe the behavior of individual nanoparticles under these experimental conditions. While testing Bi$_2$O$_3$ it was seen that the material reacted with the carbon coating of the TEM grid, again displaying a condensed phase reaction. The TEM studies provide evidence that other nanothermites may follow this mechanism as well. Furthermore, a T-Jump/PMT setup was used to optically determine the burn times and ignition temperatures in filament heating experiments, and was also used at the Argonne National Laboratory's Advanced Photon Source. This work provided unique high speed phase contrast imaging that offers further insight into the aluminum nanothermite reactions.

Introduction

Nanocomposite thermite reactions are attracting increased interest in the field of energetic materials due to high energy densities and adiabatic flame temperatures, which are comparable or greater to those of traditional organic based energetics (e.g. RDX). However, due to large characteristic diffusion length scales, traditional thermites burn at a much slower rate than those of organic energetics which have the fuel and oxidizer essentially mixed at the atomic level. Nanothermites, which are typically made with aluminum nanoparticles of size less than 100 nm, drastically reduce diffusion lengths compared to microscale particles and demonstrate burn rates up to several orders of magnitude higher.[1-5] Given the central role that nanoaluminum plays, much attention has been given to understanding the transport of aluminum with respect to its Al_2O_3 shell. If the aluminum nanoparticle is rapidly heated, the nearly instantaneous melting of the aluminum could have considerable effects in aiding of aluminum transport. The exact nature of aluminum transport is not known, but several models have been proposed including aluminum and oxygen diffusion through the alumina shell[6], pressure build up due to melting of the aluminum, which ruptures the shell allowing Al to leak out[7] and extreme pressure build up causing eruption of the alumina shell that spallates the molten aluminum[8]. Regardless of the argument, it can be agreed that rapid heating of an aluminum particle will have a positive effect on the transport of aluminum. In recent studies interest has shifted towards understanding the effect of different oxidizers on the nanothermite reaction.[9-11]

Because of the large variety of metal oxides available, each with different physical, chemical, and electrical properties, the potential to change the energy release profile becomes feasible. Our group has done some previous work characterizing nanothermite reactions.[9, 12, 13] In particular, our work has highlighted the dependence of nanothermite ignition on the gaseous oxidizer release from the metal oxides CuO, Fe_2O_3, and ZnO.[14] However, there is uncertainty as to whether oxidizer release to the gas phase is a necessary mechanistic step for all nanothermite compositions. In chemical looping combustion (CLC) systems, condensed phase reaction between carbon and CuO has been demonstrated.[15] In this work Siriwardane and co-workers suggests that the surface of the CuO, which has a Tammann of ~405 ^{o}C, melts and provides a pathway for oxygen distribution to the solid coal. There

are significant differences between the phase transitions of carbon and aluminum in the temperature ranges of a combustion system. Aluminum has a melting point of 660 $^{\circ}$C and boiling point of 2520 $^{\circ}$C, where as carbon will not change phase until over 3800 $^{\circ}$C.[16] These differences will have effects on transport properties between the two systems, but some aspects of the reaction mechanism may be transferrable.

Another metal oxide of particular interest in nanothermite formulations is bismuth trioxide, which has a relatively low vapor pressure and unique conducting properties when heated. Bi_2O_3 is well known as a good oxide ion conductor, and has been highly researched for use in electrochemical cell applications.[17-21] The δ-phase of Bi_2O_3, which is stable from 1002-1097 K [18, 21], shows an advanced ion conductivity up to two orders of magnitude greater than that of its other phases.[17] It has been observed that when combined with aluminum nanoparticles, a very reactive Bi_2O_3 nanothermite is formed. Sanders *et al* [10] investigated the difference between four different aluminum nanothermites Al/CuO, Al/Bi_2O_3, Al/MoO_3, and Al/WO_3. Each of these thermite mixtures was subjected to tests in a closed bomb pressure cell, open tray burn, and burn tube experiments. Their results show that Al/Bi_2O_3 produces the greatest peak and average pressure, as would be expected from equilibrium calculations that indicate it produces the most gaseous species during combustion when compared to other oxidizers.[10, 11, 22] However, Al/Bi_2O_3 had the lowest propagation velocity in burn tube experiments, and had a slightly lower propagation rate than Al/CuO in the open tray experiments. Differing results were seen in open tray experiments by Puszynski et al where Al/Bi_2O_3 produced higher burn rates than Al/CuO, Al/MoO_3, or Al-WO_3.[22] This group also performed DSC traces at slow heating rates of 1-20 K/min and determined the decomposition temperature to be in the range of ~839-861 K depending on the size of the Bi_2O_3 particles used in the mixture. We have also investigated the formation of ionic species during the nanothermite reaction in Al/Bi_2O_3, Al/CuO, Al/Fe_2O_3, and Al/WO_3, demonstrating that the bismuth oxide thermite produces the highest rate of ion release of the samples.[12]

Because of the interesting and in some cases contradictory behavior of the Bi_2O_3 and carbon nanocomposite systems, and the fact that no studies are available at high heating rates, we show in this paper our results at heating rates greater than 10^5 K/s, of time resolved mass-spectrometry, and high

heating rate SEM. These results suggest that both Bi_2O_3 and carbon containing nanocomposites show a primary reaction pathway that is consistent with condensed phase reactions.

Experimental

Nanocomposite samples were prepared by mixing aluminum and Bi_2O_3 nanoparticles particles to obtain a stoichiometric mixture.

$$2Al + Bi_2O_3 \rightarrow Al_2O_3 + 2Bi \qquad\qquad (1)$$
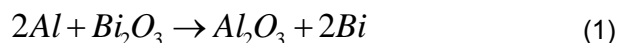
Oxidizers were purchased from Sigma Aldrich, and were spherical and agglomerated. These include Bi_2O_3 (90-210 nm), Fe_2O_3 (<50 nm), and CuO (<50 nm), with the sizes specified by the supplier. The aluminum was purchased from Argonide, Corp. and has an average particle size of ~50 nm. C/metal oxide samples were also stoichiometrically mixed. The C/Bi_2O_3 reaction is given as an example,

$$3C + 2Bi_2O_3 \rightarrow 3CO_2 + 4Bi \qquad\qquad (2)$$
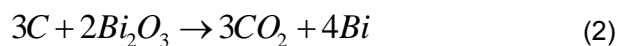
where the carbon is "regal 300" carbon black attained from Cabot Corp. When calculating stoichiometry, the Al_2O_3 shell which makes up 30% of the mass of the aluminum sample is taken into account as previously determined through thermogravimetric analysis. The samples are initially placed in a hexane solution and sonicated for ~20 min to ensure a fine mixing of materials. The primary instrument used is a Temperature-Jump/Time-of Flight Mass Spectrometer (T-Jump/TOFMS). The system and experimental procedure has been described in detail elsewhere.[23] In brief, the sample slurry is coated on a ~1 cm long, 76 µm diameter platinum filament, which can be heated at a very high rate of up to 10^6 K/s with the use of a tunable voltage pulse from an in-house built power supply. The essence of the experiment is that the T-Jump filament is directly inserted close to the electron ionization region of a custom time-of-flight mass spectrometer (MS). This allows for a very short delay (~20 µs) between product species evolution and ionization and subsequent detection by the micro-channel plate (MCP) detector of the TOFMS. Ionization of the gaseous product species is performed by an electron-impact (EI) ionization source with an energy of 70 eV. For a typical heating event, a sequence of 95 spectra with m/z (mass to

charge ratio) up to 400 are recorded with a temporal resolution of 100 µs. Furthermore, the current and voltage through the filament are simultaneously recorded during heating to determine the onsite filament temperature. The experimental procedure for our nanothermite self-ionization study is given elsewhere, [12] but in short, the setup is the same as for a normal T-Jump/TOFMS run, except that the e-gun is turned off. Therefore any ions that are detected by the MCP are strictly from ionization during the reaction.   Several experiments were conducted with the addition of simultaneous high speed imaging using a Phantom 12.1 camera for select T-Jump experiments using an imaging rate of ~33,000 fps. Aside from the nanocomposite samples, the carbon, aluminum, and metal oxide samples were each tested separately in the T-Jump/TOFMS system to investigate each material's role in the nanocomposite initiation. In a complimentary study, Al/Bi_2O_3, Al/CuO, and Al/Fe_2O_3 nanothermites were tested in a constant volume pressure cell that has its experimental details described elsewhere.[24]

A unique heating holder (Protochips, Inc.) was also used to visually investigate the morphological changes of Bi_2O_3 inside a scanning electron microscope (SEM). This holder can heat the sample in-situ from room temperature to a maximum of 1473 K, at a rate of 10^6 K/s. The before and after images can be compared to draw some conclusions about how the reaction occurred. In the context of the mass-spectrometry results we can consider this as "T-Jump microscopy".

Results and Discussion

T-Jump Mass Spectrometry

We begin our analysis by first investigating the time resolved mass spectra of the reaction products from rapid heating of Al/Bi_2O_3 and neat Bi_2O_3 nanothermite mixtures. For each case the heating rate was set to ~$5x10^5$ K/s which for a pulse time of ~3 ms, gave a final temperature of ~1870 K. It should be noted that our TOFMS has a background signal at m/z 18, (H_2O^+) and minor peaks at m/z 17, 28, and 32, representing OH^+, N_2^+, and O_2^+ respectively. A typical spectrum obtained during Bi_2O_3 heating is shown in Figure 1. It shows a peak at m/z 32 for O_2^+, m/z 44 for CO_2^+, m/z 104.5 for Bi^{+2}, m/z 209 for Bi^+, and m/z 216 for BiOH. A full time-resolved set of spectra of the Al/Bi_2O_3 reaction is shown in Figure 2 where each spectrum is separated by 100 µs. The detailed Al/Bi_2O_3 spectrum in Figure 3 shows

peaks at Al^+, Bi^+, Bi^{+2}, O_2^+, and CO_2^+. One interesting feature not observed in our mass spectral

characterization of other thermites is the doubly charged Bi in the Bi2O3 system.[9, 12] This is likely due

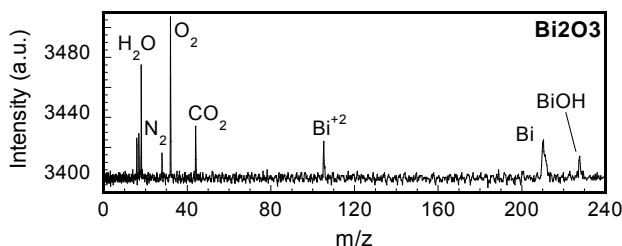to Bismuth having low first and second ionization potentials of ~7.29 and 16.69 eV respectively.[25]

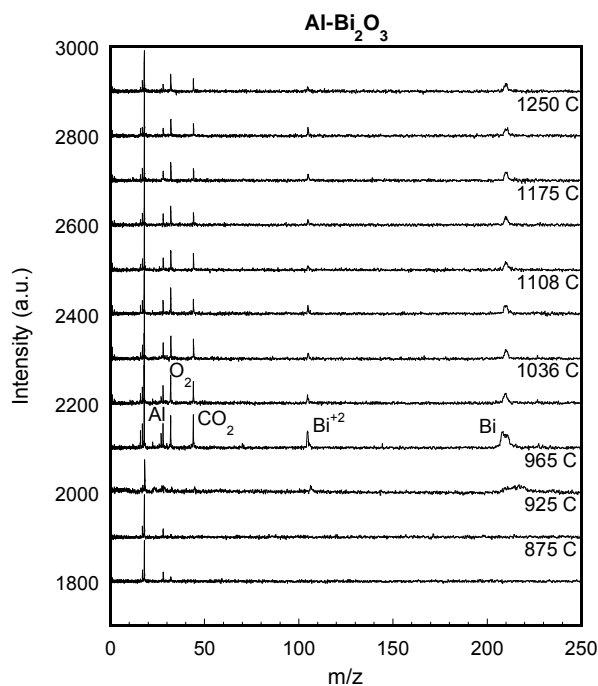**Figure 1:** Time-of-flight mass spectrum for Bi_2O_3 sample.

Figure 2: Full spectrum for Al-Bi_2O_3 nanothermite reaction. Each spectrum is separated in time   by 100 μs.

Our self-ionization work also demonstrated unique ion formation properties for the Bi_2O_3 thermite as it had

a higher ionization rate than the other thermites tested.[12] Another interesting feature of Al/Bi_2O_3

nanothermite is the amount of Bi vapor formed compared with metal vapor formed in other reactions. If

Bi_2O_3 goes through reaction (1), then Bi would be in gas phase due to its relatively low boiling

temperature of 1837 K and an adiabatic flame temperature for the system of 3253 K.[25, 26] Al/CuO and

Al/Fe$_2$O$_3$ reactions form very high temperature boiling metals (Cu: 2835 K; Fe: 3134 K) [25], and have

adiabatic flame temperatures of 2843 K and 3135 K respectively, thus we should expect more vapor

phase Bi. This trend can be confirmed through comparison of Al/Bi$_2$O$_3$, and Al/CuO systems in Figure 4,

which shows bismuth and copper gas release from their respective nanothermite systems during T-

Jump/MS experiments.
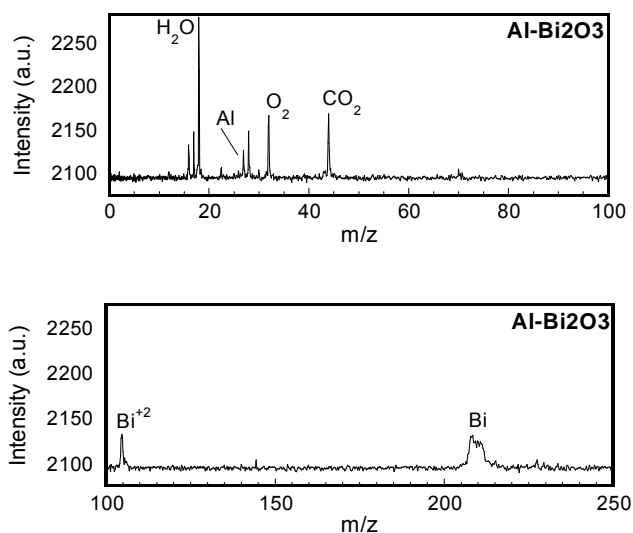
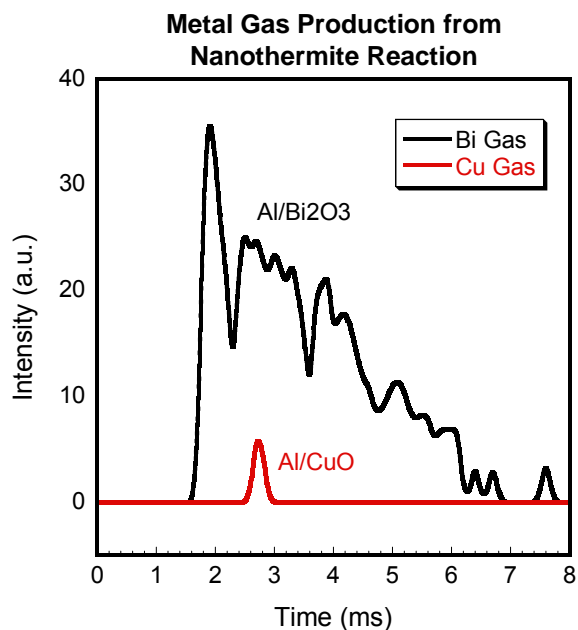**Figure 3:** Time-of-flight mass spectrum for Al/Bi$_2$O$_3$ sample (TOP: m/z 0-100, BOTTOM: m/z 100-200).

Figure 4: Bi and Cu gas release from Al/Bi$_2$O$_3$ and Al/CuO nanothermites.

To further investigate the nature of Al/Bi$_2$O$_3$ combustion, high speed imaging was used to capture the nanothermite reaction while simultaneously sampling with the T-Jump/MS. Figures 5 and 6 show selected images of the T-Jump experiments under vacuum for Al/Bi$_2$O$_3$ and Al/CuO respectively at a framing rate of ~33,000 fps (every 30 s). From these images we concluded that Al/Bi$_2$O$_3$ burns about twice as fast as Al/CuO as these samples had burn times of ~0.09 ms and ~0.18 ms, respectively.
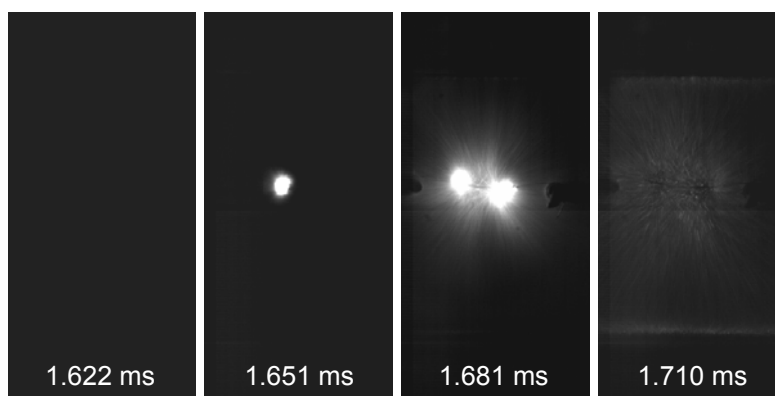

| 1.622 ms | 1.651 ms | 1.681 ms | 1.710 ms |

Figure 5: High speed images of Al/Bi$_2$O$_3$ during heating in the TOFMS.

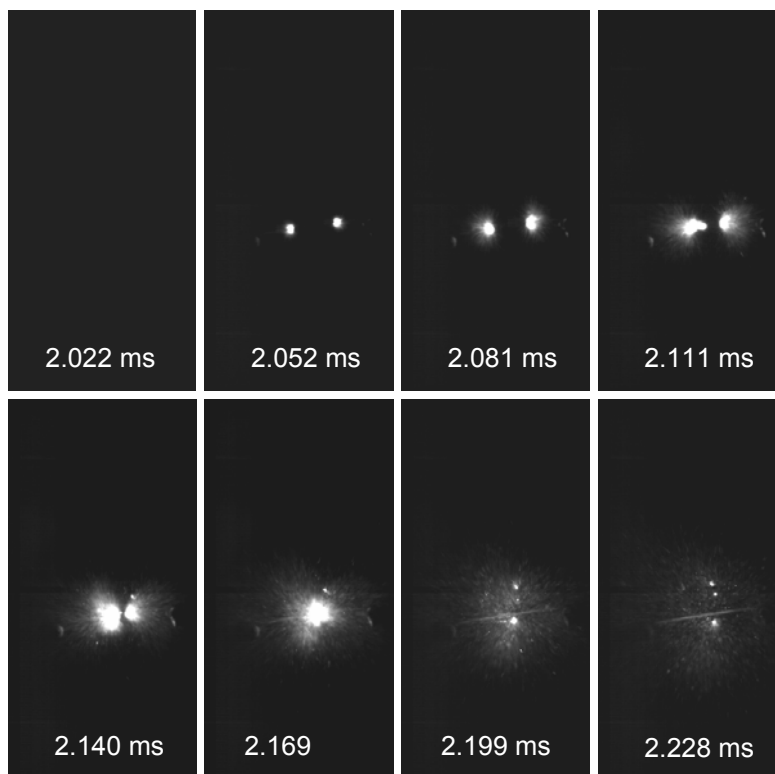| 2.022 ms | 2.052 ms | 2.081 ms | 2.111 ms |
| 2.140 ms | 2.169 | 2.199 ms | 2.228 ms |

Figure 6: High speed images of Al/CuO during heating in the TOFMS.

Previous burn tube and open tray experiments testing thermite performance have given mixed results as to whether Al/CuO or Al/Bi$_2$O$_3$ exhibits a higher burn rate because of the difficulty in controlling experimental parameters. Packing density, particle size, tube diameter, and pressure are just a few critical experimental parameters that greatly influence burn rate results. For comparison in this paper, we consider the work by Son and co-workers on aluminum nanothermites of CuO, Bi$_2$O$_3$, MoO$_3$, and WO$_3$ in both open tray and burn tube setups.[10] Their results show that Al/CuO has the fastest burn rate in open tray experiments followed by Al/Bi$_2$O$_3$, while in the burn tube, Al/Bi$_2$O$_3$ was the poorest performer followed by Al/CuO. So in both the burn tube and open tray experiment Al/CuO outperformed Al/Bi$_2$O$_3$, however, in our filament tests it is clear that the opposite is true.   To resolve this discrepancy we refer to the work of Weismiller *et al* who reported on the dependence of pressure and atmosphere on Al/CuO in a burn tube experiment.[27] They reported that higher pressures have a significantly detrimental effect on the burn velocity of a nanothermite ,and ascribed this as a shift from a convective mode of heat transfer to a conductive one with an increase in pressure.[27] We can compare those results with our pressure cell data in Table 1, which shows maximum pressure, pressure rise time, pressurization rate, and overall burn time, for various nanothermite composites. Clearly Al/Bi$_2$O$_3$ has the highest maximum pressure followed by Al/CuO and Al/Fe$_2$O$_3$. This result, which has also been reported in other works, corresponds to the predicted high gas release for Al/Bi$_2$O$_3$.[26] In burn tube experiments it is reasonable to believe that the slower burn rate for the bismuth thermite is due to the increased local pressure while burning, which shifts the heat transfer to a conductive mode. The thermite reaction in the mass spectrometer is at a much lower pressure and thus as expected, the reaction in the bismuth oxide system is more rapid.

Table 1: Pressure cell results for various nanothermites.

Sample	Pmax (psi)	Pressure Rise Time (µsec)	Pressurization Rate (psi/µsec)	Burn Time (µsec)

Al/Bi$_2$O$_3$	157	10.0	15.7	197
Al/CuO	98	8.8	11.1	170
Al/Fe$_2$O$_3$	13.4	800	.017	936

The temporal nature of the T-Jump mass-spectrometer experiment allows us to draw some conclusions about the initiation steps that may be involved with the bismuth nanothermite and how it differs from some other systems. In our previous work, we studied the nanothermite reaction of Al/CuO, Al/Fe$_2$O$_3$, and Al/ZnO.[9] For each of these materials we investigated the decomposition of the thermite, as well as decomposition of the metal oxide and aluminum nanopowders.
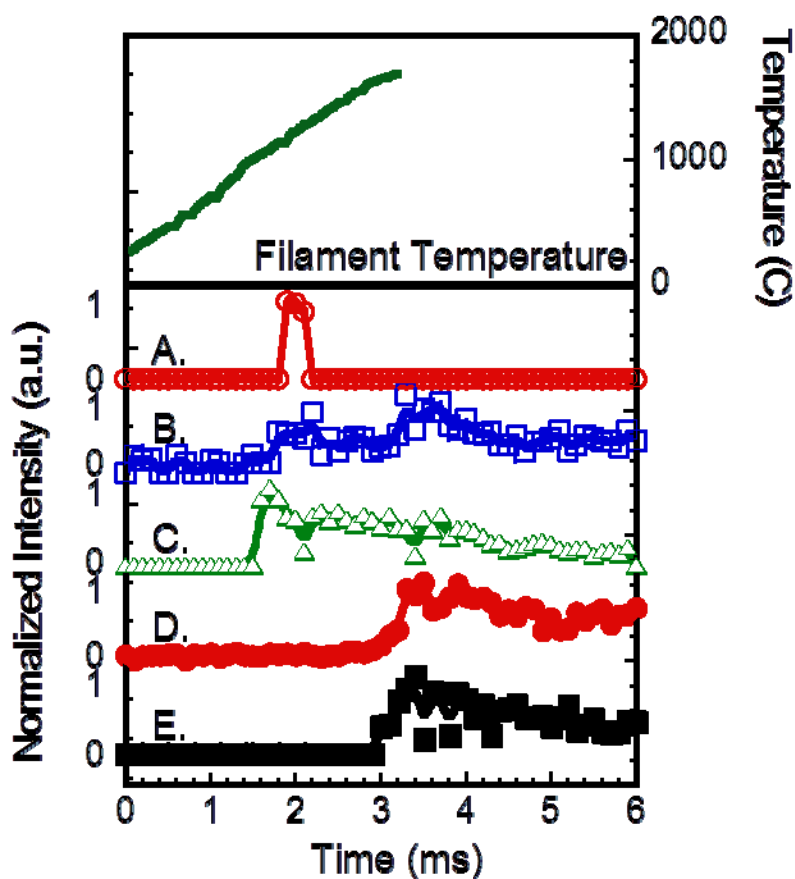

Figure 7: (A-C) Products from Al/Bi$_2$O$_3$. (D-E) Products from Bi$_2$O$_3$. (A) Al, (B) O$_2$, (C) Bi, (D) O$_2$, (E) Bi.

We found from comparing the metal oxide spectra and the thermite spectra that the thermite reaction initiates at a time in close proximity to the point of release of gaseous O_2 from the respective oxidizer. In comparison, Al/Bi_2O_3 shows a much different reaction characteristic. Figure 7 shows the filament temperature, as well as reaction product concentrations as detected by the mass spectrometer for Al/Bi_2O_3, and Bi_2O_3 in the current study. If we compare the reaction products in Figure 7 from the thermite (parts A-C) and the oxide (parts D-E) heating, we see that unlike other nanothermites, there is a significant difference in times between thermite ignition, and gas phase O_2 release from the oxide. Although these two samples were tested in separate heating runs, the experimental conditions were replicated in a similar fashion so that qualitative conclusions can be confidently made. We see that when the oxide is heated by itself, Bi and O_2 are released very late at ~3.1 ms and T = 1940 K. This compares to the thermite case where combustion starts at ~1.6 ms and T = 1273 K, as signified by the appearance of Bi, O_2, and shortly after, Al. Clearly, unlike the iron oxide and copper oxide thermite reaction systems, where ignition occurs very close to the point that the oxide releases gaseous O_2, the initiation of the Al/Bi_2O_3 occurs before the Bi_2O_3 decomposes to release gaseous oxygen. This evidence strongly suggests that the initiation of the Al/Bi_2O_3 reaction occurs in the condensed phase.

To further investigate this mechanism we consider a fuel which cannot vaporize at these temperatures. For this purpose we employ a C/Bi_2O_3, C/CuO, and C/Fe_2O_3, composites using nanometer scale carbon particles. To observe reaction within this system, the only feasible reaction pathway is for the oxygen from the oxide to heterogeneously react with the carbon particles.
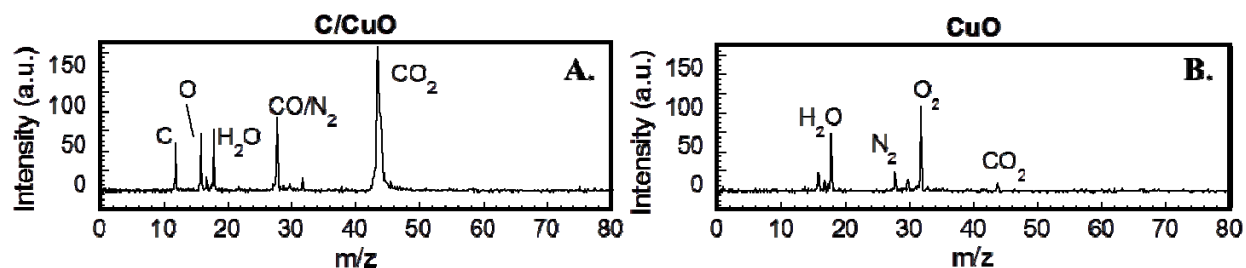

Figure 8: Individual spectra for A. C/CuO, and B. CuO

.

To investigate the reaction products from rapid heating of the carbon nanocomposites, the neat metal oxides and nanocomposites were individually heated in separate experimental runs. Figures 8a and 8b show individual detailed spectra for the nanocomposite C/CuO, and the neat oxide CuO, respectively. A typical background spectrum for our mass spectrometer consists of peaks at mass to charge ratios (m/z) 18 (H_2O) and 28 (N_2), with smaller peaks at m/z 32 (O_2) and 17 (OH). The main reaction product for the carbon nanocomposite combustion in vacuum is CO_2 (m/z 44) as can be seen in both Figure 8a. There are several smaller peaks observed at m/z 12 (C) and 16 (O) as well as an increase in m/z 28 (CO), which are all considered to be due to fragmentation of the CO_2 molecule during ionization. This corresponds well to what is reported for the CO_2 mass spectrum in the NIST spectral library.[28] The small peaks at m/z 32 (O_2) are due to a small amount of oxygen not consumed in the reaction that is released to the gas phase. For the neat nanopowder, there is a significant difference in the amount of CO_2 and O_2 as compared to the nanocomposite. In Figure 8b the intensity of O_2 is greater than that in the nanocomposite, and the CO_2 is substantially decreased. This trend was also confirmed for the C/Bi_2O_3 and C/Fe_2O_3 nanocomposites. It is clear from comparison of the nanocomposites vs. neat oxide nanopowders that the O_2 formed by the metal oxides is almost entirely consumed in the reaction with carbon to form CO_2.
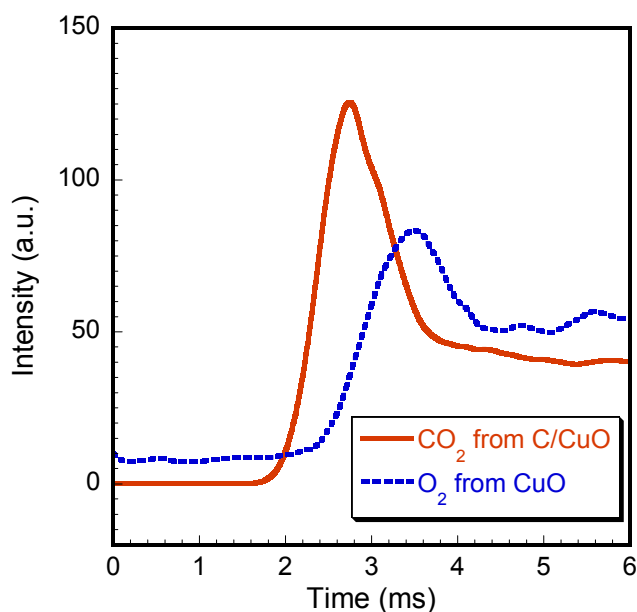

Figure 9: Detected CO_2 and O_2 concentration from C/CuO and CuO, respectively.

With carbon dioxide detected as the prominent gaseous product species, it is unclear how the carbon is oxidized to form this. To further investigate the reaction pathways, comparison is made between time-resolved concentration profiles for the neat metal oxide nanopowders and the nanocomposites. The oxygen release profile from the neat copper oxide is compared with the carbon dioxide release from the C/CuO nanocomposite in Figure 9.
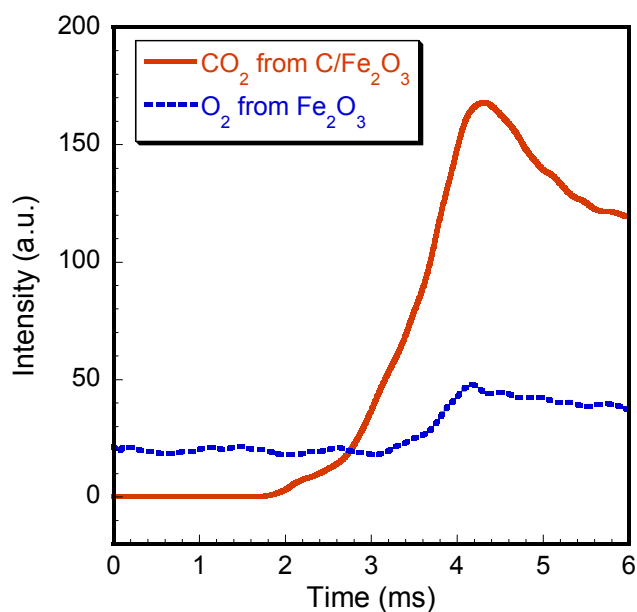

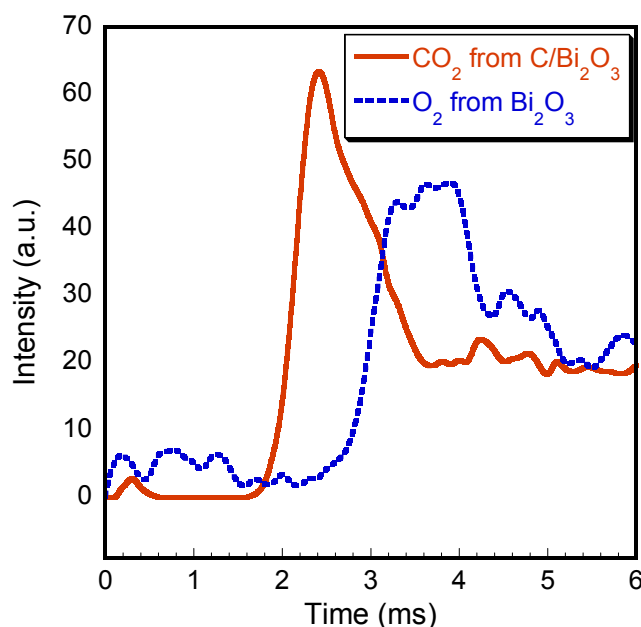**Figure 10:** Detected CO_2 and O_2 concentration from C/Fe_2O_3 and Fe_2O_3, respectively.

Figure 11: Detected CO_2 and O_2 concentration from C/Bi_2O_3 and Bi_2O_3, respectively.

This gives a correlation between what time/temperature the O_2 is released from the oxide, and when the reaction starts to progress in the C/CuO nanocomposite. From Figure 9 it can be seen that the CO_2 is produced from the C/CuO at a lower temperature than O_2 is released to the gas phase from the CuO. This strongly suggests that there is a condensed phase reaction mechanism driving the CO_2 producing reaction. Figure 10 plots the CO_2 production from C/Fe_2O_3 along with the O_2 release from Fe_2O_3, and Figure 11 does the same for Bi_2O_3. This Figure shows the same trend as that for C/CuO, the carbon dioxide is produced well before gaseous O_2 is available, therefore the initiation of this reaction must be in the condensed phase.

T-Jump Microscopy

To further explore the idea of a condensed phase combustion mechanism, we investigate the morphological changes, using in-situ rapid heating within a scanning electron microscope (SEM, Hitachi SU-70). The sample grids, which have a few nanometer thick holey carbon film deposited over a silicon carbide substrate, offer the opportunity to study the heating of Bi_2O_3 as well as the reaction with the

underlying carbon substrate.   Figure 12 shows an SEM image of the sample on the grid before heating. The dark background is the thin carbon film, and the grainy looking areas are the holes in the carbon film which expose the underlying silicon carbide. The Al/Bi_2O_3 was sparsely placed on the grid so that in certain instances the Bi_2O_3 and Al are isolated as shown in Figure 12.

The sample was given a heating pulse from room temperature to 1250 K at a rate of 10^6 K/s, and then held for 1 ms the results of which are shown in Figure 13. Elemental analysis of the sample after heating is shown in Figure 14. Despite the fact that we were well above the melting point of aluminum, it is clear that the aluminum aggregate did not undergo any sintering. However, the Bi_2O_3 showed significant changes within the 1 ms timescale of the heating pulse. It should be noted that with a longer heating pulse the aluminum will also show significant morphological change. One would expect that since aluminum melts at 933 K and bismuth trioxide melts at 1097 K that we would see some changes in aluminum before Bi_2O_3. These results suggest that either the timescale of heat conduction is significantly lower in Al than in Bi_2O_3, or that the alumina shell is not immediately rupturing upon melting of the aluminum core. Figure 14 confirms that during heating the Bi_2O_3 forms a film of Bi_2O_3 with spheres of Bi on its surface. If we consider regions where Bi_2O_3 is only in contact with the carbon film but not near any aluminum we can observe a region where we have a Bi_2O_3 film over which a much larger elemental Bi particle sits.
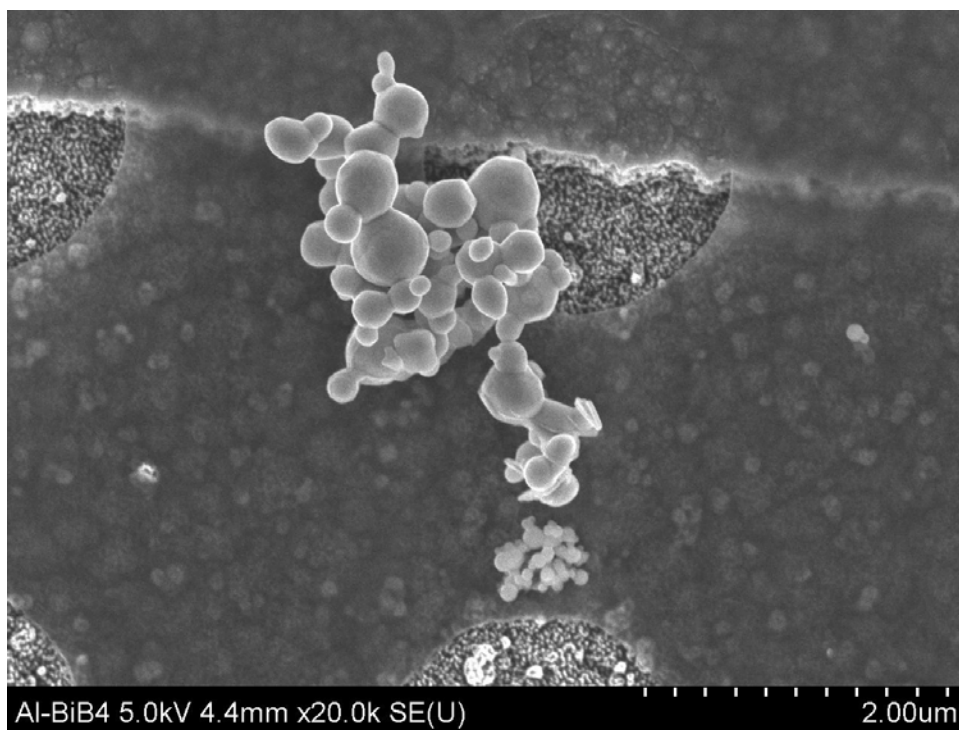
Figure 12: TEM image of bismuth trioxide and aluminum nanoparticles before heating.

This strongly suggests that the Bi_2O_3 liquid reacts with the carbon which can be indicated by the recession of the hole in the carbon film from Figure 12 to Figure 13. The C/Bi_2O_3 reaction produces liquid Bi (MP 545 K), which appears to be immiscible in liquid Bi_2O_3 allowing it to phase separate and form larger spherical particles. This result appears to be highly consistent with the condensed phase reaction model deduced from the T-Jump/TOFMS experiments.. The fact that the liquid Bi_2O_3 melts and wets the surface of the carbon further suggests that there is a transfer of oxygen through the liquid Bi_2O_3 phase.

We also note that the reaction has proceeded to completion within the timescale of the heating pulse, <1 ms. The reaction may have actually occurred even faster, however, 1 ms was the minimum pulse which could be applied. This may imply that very thin carbon is a viable fuel to use in a thermite formulation, so long as the length scales are sufficiently small and the oxidizer can heterogeneously react with carbon.
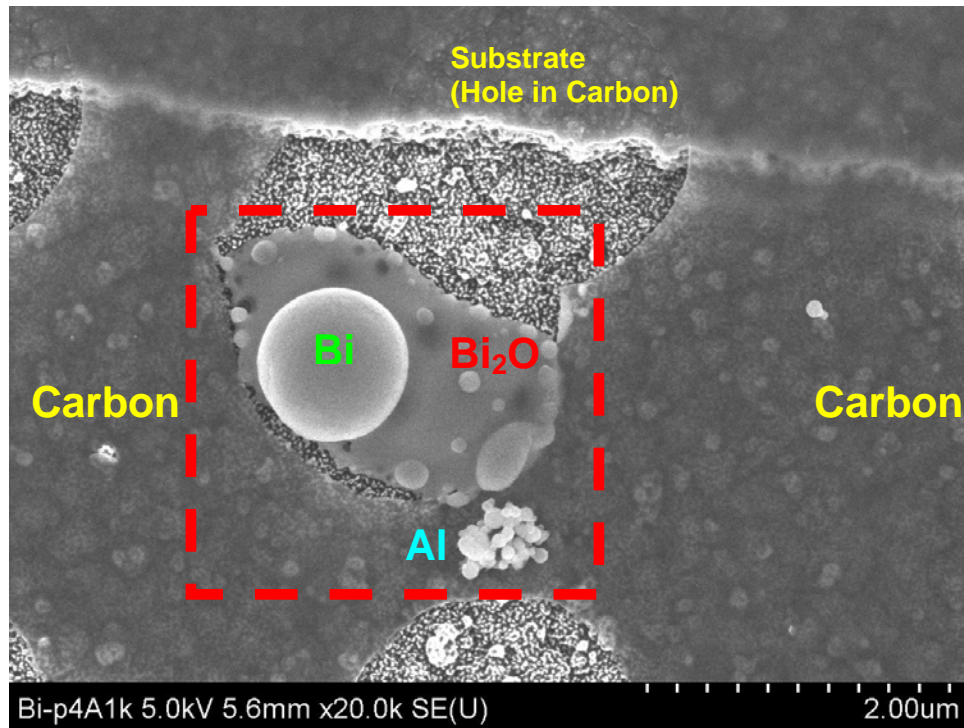
Figure 13: TEM image of Bi_2O_3 and Al particles after heating with high heating rate TEM grid. Dotted box represents area sampled by EDS shown in Figure 14.

If carbon could be utilized as a fuel, then much higher overpressures could be realized via the formation of a gaseous CO_2 product, thus greatly improving the performance. Carbon is also unique in that it will not have a passivating oxide shell like that of metal surfaces. With no oxide shell, there would be no loss of mass due to partial oxidation, but also, there should be little to no ignition delay caused by diffusion of species through the shell, as has been reported for nano-Al.[13] As a performance test a C/Bi_2O_3 sample was placed in the pressure cell, but the sample failed to initiate. It is possible that this was due to high agglomerate particle size, despite primary particles being on the order of 10's of nanometers. Despite this failed test, the lack of a passivating shell, and high possible pressure outputs make carbon an attractive additive to metals, however, much more work will have to be done to test its viability.
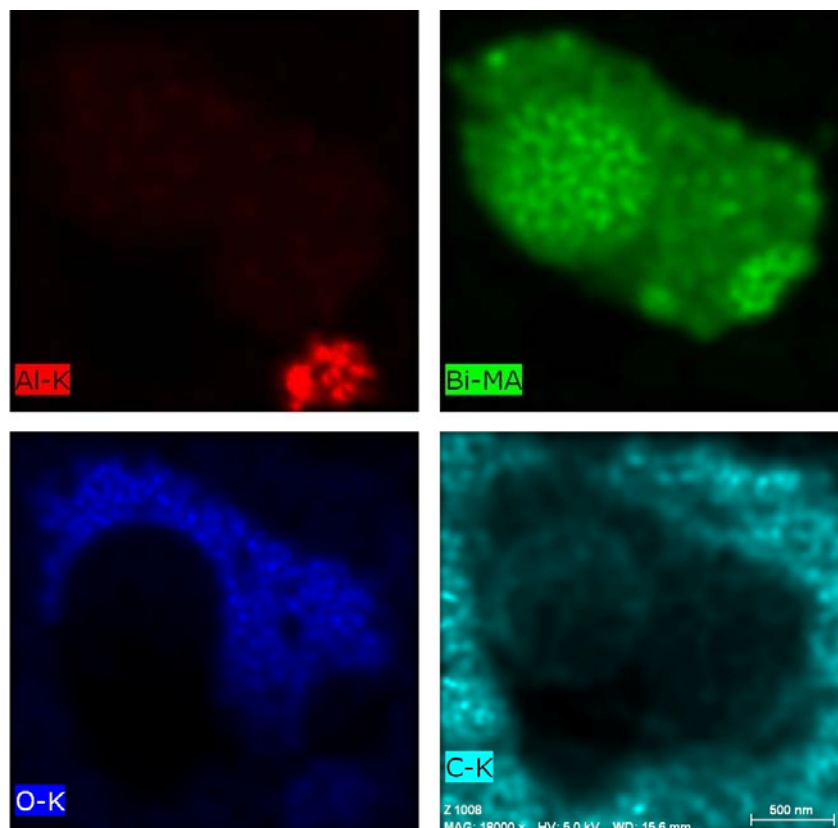
Figure 14: Elemental analysis of boxed region in Figure 13.

<u>Discussion</u>

In our previous works, the difference in ignition points for various aluminum thermites suggests a strong dependence on the oxidizer for triggering the ignition point.[14] It is likely that for the Al/CuO and Al/Fe$_2$O$_3$ nanothermites, which ignite at higher temperatures than Al/Bi$_2$O$_3$, the aluminum was already exposed at the time of oxygen release from the oxidizer. Bi$_2$O$_3$ will likely have free O^{2-} ions within its lattice as soon as it enters its ion conducting phase at 1002 K, just above the melting point of aluminum at 933 K. If we take into account our high heating rate, this temperature change will happen on the order of 10 μs. Our temperature for ignition of the bismuth oxide thermite is determined to be slightly higher in temperature than the δ-phase transition in Bi$_2$O$_3$, however, this high ignition temperature could be a result of implementing such a high heating rate. Our ignition temperature for Al/Bi$_2$O$_3$ is also higher than that reported by other groups. From Figure 7 we determine the temperature at ignition to be the point where

reaction products are first observed at ~1273 K, while Puszynski observed an exotherm in the Al/Bi$_2$O$_3$ reaction at temperatures of ~839-861 K. At this point we are not able to resolve this discrepancy but it is clear that we are probing different reaction kinetics than most of the previous works. High heating rates clearly result in a much more rapid exothermic event as compared to the slower heating rate studies which show a broad temporal exotherm.[22] Slow heating rates apparently also allow for the reaction to start at a temperature below the melting point of Al. Since the aluminum remains in the solid phase, the reaction is likely limited by the diffusion of oxygen through the Al$_2$O$_3$ shell.[6] If we take the case for the bismuth oxide sample, if a high heating rate is applied, once the temperature reaches the point where the δ-phase is reached, we suddenly have an abundance of free, mobile oxygen ready to react, as well as aluminum in the liquid phase which can diffuse out of the Al$_2$O$_3$ shell.

This mechanism can be combined with our recently proposed reactive sintering mechanism,[29] and can also be applied to the carbon nanocompsites. In our previous T-Jump microscopy experiment with an Al/WO$_3$ nanothermite, we observed that during certain heating pulses neat WO$_3$ would undergo little to no morphological changes. However, under the same heating pulse, when the WO$_3$ was in contact with aluminum, significant melting of the WO$_3$ occurred. We believe that a condensed phase exothermic reaction between the Al and WO$_3$ aided in the heating of the material and caused these morphological changes. For the carbon based reactions this is likely a similar mechanism, where reactive sintering creates an intimate contact between the fuel and oxidizer to allow for a rapid condensed phase reaction. This also corresponds with the prediction by Siriwardane that the surface of the metal oxide particle can melt at the Tammann temperature, and create a pathway for oxide transfer to the fuel.[15] This would explain the reactions occurring in the condensed phase before the gaseous oxidizers are released.

Conclusion

T-Jump/TOFMS experiments were used to investigate the initiation and reaction of various aluminum and carbon nanocomposites. Time resolved spectra were compared with those from previous nanothermite studies as well as spectra of the neat oxides and fuels. It was observed that both aluminum and carbon nanocomposites react well before gaseous oxygen release from the oxide, and all evidence

points to a condensed phase initiation of the reaction. This was also confirmed by heating rate SEM experiments where the Bi_2O_3 oxide reacted with the carbon film of the SEM grid. It was also seen that bismuth oxide nanothermites reacted faster than copper oxide nanothermites within our T-Jump/MS experiments. This suggests that the condensed phase initiation reactions in nanocomposites are capable of being extremely rapid.

Acknowledgment

References

[1] J.A. Puszynski, Processing and characterization of aluminum-based nanothermites, Journal of Thermal Analysis and Calorimetry, 96 (2009) 677-685.
[2] S.F. Son, R.A. Yetter, V. Yang, Introduction: Nanoscale composite energetic materials, Journal of Propulsion and Power, 23 (2007) 643-644.
[3] G.M. Dutro, R.A. Yetter, G.A. Risha, S.F. Son, The effect of stoichiometry on the combustion behavior of a nanoscale Al/MoO3 thermite, Proceedings of the Combustion Institute, 32 (2009) 1921-1928.
[4] F. Shimojo, A. Nakano, R.K. Kalia, P. Vashishta, Enhanced reactivity of nanoenergetic materials: A first-principles molecular dynamics study based on divide-and-conquer density functional theory, Applied Physics Letters, 95 (2009).
[5] V.I. Levitas, M.L. Pantoya, B. Dikici, Melt dispersion versus diffusive oxidation mechanism for aluminum nanoparticles: Critical experiments and controlling parameters, Applied Physics Letters, 92 (2008).
[6] A. Rai, K. Park, L. Zhou, M.R. Zachariah, Understanding the mechanism of aluminium nanoparticle oxidation, Combustion Theory and Modelling, 10 (2006) 843-859.
[7] V. Rosenband, Thermo-mechanical aspects of the heterogeneous ignition of metals, Combustion and Flame, 137 (2004) 366-375.
[8] V.I. Levitas, B.W. Asay, S.F. Son, M. Pantoya, Melt dispersion mechanism for fast reaction of nanothermites, Applied Physics Letters, 89 (2006).
[9] L. Zhou, N. Piekiel, S. Chowdhury, M.R. Zachariah, Time Resolved Mass Spectrometry of the Exothermic Reaction between Nanoaluminum and Metal Oxides: The Role of Oxygen Release, SUBMITTED, (2010).
[10] V.E. Sanders, B.W. Asay, T.J. Foley, B.C. Tappan, A.N. Pacheco, S.F. Son, Reaction propagation of four nanoscale energetic composites (Al/MoO3, Al/WO3, Al/CuO, and Bi2O3), Journal of Propulsion and Power, 23 (2007) 707-714.

[11] K.S. Martirosyan, L. Wang, A. Vicent, D. Luss, Synthesis and performance of bismuth trioxide nanoparticles for high energy gas generator use, Nanotechnology, 20 (2009).

[12] L. Zhou, N. Piekiel, S. Chowdhury, D. Lee, M.R. Zachariah, Transient ion ejection during nanocomposite thermite reactions, Journal of Applied Physics, 106 (2009).

[13] S. Chowdhury, K. Sullivan, N. Piekiel, L. Zhou, M.R. Zachariah, Diffusive vs. Explosive Reaction at the Nanoscale, J. Phys. Chem. Lett. in press, (2010).

[14] L. Zhou, N. Piekiel, S. Chowdhury, M.R. Zachariah, Time-Resolved Mass Spectrometry of the Exothermic Reaction between Nanoaluminum and Metal Oxides: The Role of Oxygen Release, Journal of Physical Chemistry C, 114 (2010) 14269-14275.

[15] R. Siriwardane, H.J. Tian, D. Miller, G. Richards, T. Simonyi, J. Poston, Evaluation of reaction mechanism of coal-metal oxide interactions in chemical-looping combustion, Combustion and Flame, 157 (2010) 2198-2208.

[16] NIST Standard Reference Database 69: *NIST Chemistry WebBook*, U.S. Secretary of Commerce on behalf of the United States of America, 2008.

[17] S. Hull, S.T. Norberg, M.G. Tucker, S.G. Eriksson, C.E. Mohn, S. Stolen, Neutron total scattering study of the delta and beta phases of Bi2O3, Dalton Trans., (2009) 8737-8745.

[18] P. Shuk, H.D. Wiemhofer, U. Guth, W. Gopel, M. Greenblatt, Oxide ion conducting solid electrolytes based on Bi2O3, Solid State Ionics, 89 (1996) 179-196.

[19] A.C.S. Sabioni, A. Daniel, W.B. Ferraz, R.W.D. Pais, A.M. Huntz, F. Jomard, Oxygen Diffusion in Bi2O3-doped ZnO, Materials Research-Ibero-American Journal of Materials, 11 (2008) 221-225.

[20] T. Ivetic, M.V. Nikolic, M. Slankarnenac, M. Zivanov, D. Minic, P.M. Nikolic, M.M. Ristic, Influence of Bi2O3 on microstructure and electrical properties of ZnO-SnO2 ceramics, Science of Sintering, 39 (2007) 229-240.

[21] T. Takahashi, T. Esaka, H. Iwahara, Oxide Ion Conduction in Sintered Oxides of Moo3-Doped Bi2o3, Journal of Applied Electrochemistry, 7 (1977) 31-35.

[22] J.A. Puszynski, C.J. Bulian, J.J. Swiatkiewicz, Processing and ignition characteristics of aluminum-bismuth trioxide nanothermite system, Journal of Propulsion and Power, 23 (2007) 698-706.

[23] L. Zhou, N. Piekiel, S. Chowdhury, M.R. Zachariah, T-Jump/time-of-flight mass spectrometry for time-resolved analysis of energetic materials, Rapid Communications in Mass Spectrometry, 23 (2009) 194-202.

[24] K. Sullivan, M.R. Zachariah, Simultaneous Pressure and Optical Measurements of Nanoaluminum Thermites: Investigating the Reaction Mechanism, Journal of Propulsion and Power In Press, (2010).

[25] D.R. Lide, CRC Handbook of Chemistry and Physics, 2002.

[26] S.H. Fischer, M.C. Grubelich, Theoretical Energy Release of Thermites, Intermetallics, and Combustible Metals, 24th International Pyrotechnics Seminar, (1998).

[27] M.R. Weismiller, J.Y. Malchi, R.A. Yetter, T.J. Foley, Dependence of flame propagation on pressure and pressurizing gas for an Al/CuO nanoscale thermite, Proceedings of the Combustion Institute, 32 (2009) 1895-1903.

[28] A. Mikaia, V. Zaikin, J. Little, D. Zhu, C. Clifton, D. Sparkman, NIST/EPA/NIH Mass Spectral Library, in, Standard Reference Data Program of the National Institute of Standards and Technology, 2005.

[29] K.T. Sullivan, W.A. Chiou, R. Fiore, M.R. Zachariah, In situ microscopy of rapidly heated nano-Al and nano-Al/WO3 thermites, Applied Physics Letters, 97.

[30] B.J. Henz, T. Hawa, M.R. Zachariah, On the role of built-in electric fields on the ignition of oxide coated nanoaluminum: Ion mobility versus Fickian diffusion, Journal of Applied Physics, 107.

[31] V.P. Zhdanov, B. Kasemo, Cabrera-Mott kinetics of oxidation of nm-sized metal particles, Chemical Physics Letters, 452 (2008) 285-288.